Molecular Physics, Vol. 103, No. 6–8, 20 March–20 April 2005, 883–890

Taylor & Francis
Taylor & Francis Group

A density functional theory study of adsorbate-induced work function change and binding energy: Olefins on Ag(111)

M.-L. BOCQUET†, A.M. RAPPE‡ and H.-L. DAI‡*

†Ecole Normale Supérieure, Lyon, France
‡University of Pennsylvania, Philadelphia, USA

(*Received 26 July 2004; accepted 18 September 2004*)

The change of work function of the Ag (111) surface induced by the physisorption of ethylene and its derivatives, vinyl chloride and butadiene, is examined with density functional theory (DFT) calculations employing a generalized gradient approximation for the exchange correlation functional. It is found that the calculations can generate optimized adsorption structures in agreement with experiment, although as expected the calculation does not compute the small binding energies accurately. This DFT approach, however, predicts the work function change induced by adsorption reasonably well. Since there appears an empirical correlation between the measured adsorption energy and the calculated work function change for the studied olefins that can be justified by molecular orbital interactions, the work function changes computed within DFT may be used as a relative calibration for binding energies in physisorbed systems.

1. Introduction

A fundamental understanding of the nature of the interactions between metallic surfaces and organic compounds is important to a variety of fields that involve molecules at interfaces, such as heterogeneous catalysis and tribology. These interactions can be qualitatively separated into two regimes according to the bonding strength: chemisorption and physisorption. Chemisorption is characterized by covalent or charge transfer bonds. Physisorption, on the other hand, is generally believed to result from long-range electrostatic interactions. As the vast majority of molecule–metal interactions are of this kind and since physisorption states often exist as precursors for strongly bonded chemisorption systems, it is important to be able to deal theoretically with these weak interactions on surfaces.

Density functional theory (DFT) methods within the local density approximation (LDA) or generalized gradient approximation (GGA) have been successful in studying chemisorbed species, because of their effectiveness in treating short-range electron correlation. Numerous DFT studies have been performed to describe molecular chemisorption on noble metals such as copper [1]. The study of physisorbed species by DFT, on the other hand, constitutes another set of challenges. Because of the weak interactions involved in physisorption, there is an apparent need to properly treat long-range electronic correlations [2].

As theorists continue to extend DFT methods in order to treat long-range interactions properly [3, 4, 5], including efforts based on meta-GGA approach that showed promise in calculating physisorption energy more accurately [6], we would like to explore whether other observables accessible within standard DFT calculations can provide useful insight into the weak bonds. An experimental correlation has recently been revealed between work function changes and desorption energies for polar molecules on metals, with larger induced work function changes correlating to higher desorption temperatures [7]. Since the work function can be reliably provided by DFT calculations, this observation suggests that DFT evaluations of adsorbate induced work function change may offer a suitable approach for estimating the binding strengths of physisorbed molecules.

We have chosen the adsorption of three related organic molecules, vinyl chloride, ethylene, and butadiene, on the Ag(111) surface as the systems for study since experimental characterization of their adsorption structure and energy, has been conducted. These adsorption characteristics can be used to compare with the results from the DFT calculations and gauge the quality of the calculations. Subsequently the calculations can be used to produce the work function changes for comparison with the binding energies.

*Corresponding author. e-mail: dai@sas.upenn.edu

Molecular Physics
ISSN 0026–8976 print/ISSN 1362–3028 online © 2005
Taylor & Francis Group Ltd
http://www.tandf.co.uk/journals
DOI: 10.1080/00268970412331333609

The adsorption structure and energy of vinyl chloride (VC) on Ag(111) have been determined through temperature desorption spectroscopy and high-resolution electron energy loss spectroscopy (HREELS) [8]. Similar information on ethylene and butadiene has been ascertained previously [9] and confirmed recently [8]. All three molecules adsorb on Ag(111) at low temperatures in physisorbed states. Ethylene adsorbs on Ag(111) molecularly below 128 K through a weak bond involving π electrons with no detectable carbon hybridization. VC and butadiene adsorb at temperatures below 110 K and 166 K, respectively, with their gas phase structure unperturbed upon adsorption [8]. Unlike ethylene and butadiene which adsorb in a flat geometry, VC adsorbs with its molecular plane somewhat tilted from the surface by $\theta = 26^\circ$, with the $-CH_2$ group lying closer to the surface. Furthermore, the plane rotates around the C–C axis by $\alpha = 33^\circ$, indicating that the centre of the chlorine atom lies farthest away from the surface [8]. This adsorption geometry reflects the importance of the various factors affecting the adsorption structure of a physisorbed molecule, including bonding interactions, steric effects, and inter-adsorbate interactions. Furthermore, in thermal desorption measurements using the Redhead method [10] and a pre-exponential frequency factor of 10^{13}, the desorption energies for ethylene, VC and butadiene were determined as 7.7, 7.4 and 10.4 kcal mol^{-1}, within a few kcal mol^{-1} uncertainty [11].

There have been a few previous theoretical studies using *ab initio* methods and small silver clusters [12, 13, 14] or periodic slabs modeled with a tight binding approach [15] on olefins on silver. The tight-binding slab calculations of the (110) surface are instructive for understanding the different bonding mechanisms on a noble metal like silver in comparison with a more active metal like platinum [15]. The cluster calculation [12] showed that removal of one electron from the cluster causes the originally repulsive ethylene to bind to the cationic cluster with a binding energy of 8.7 kcal mol^{-1}. This calculation suggests an interpretation of the experimental observation [16] that ethylene readily adsorbs on oxygen-covered surfaces, presumably resembling more the Ag_3^+ cluster, but not clean silver surfaces at ambient temperatures. Very recently, *ab initio* periodic slabs calculations have been performed for ethylene on Ag(001) [17]. This GGA calculation produced a low binding energy of $\sim$2–3 kcal mol^{-1} and a molecular geometry almost unaffected by adsorption.

In this study, we examine the adsorption geometries and binding energies of olefins on a perfect Ag(111) surface using the DFT approach. First, we will show that the calculations do produce weak interactions with the correct geometry, although the calculated binding energies, as expected, are much smaller than experimental values for all the olefins. However, we show that adsorption induced work function change at the surface can be accurately calculated by DFT and used for evaluating, at least on a relative scale, the binding energy of physisorbed systems.

2. Theoretical calculations

2.1. *Computational approach and test calculations*

Calculations are performed using the VASP (Vienna Ab initio Simulation Program) [18] code. This first-principles DFT approach utilizes a plane-wave basis set, ultra-soft pseudopotentials [19] and the PW91 GGA [20]. We find the lattice constant for bulk silver to be 4.16 Å, 2% over the experimental value of 4.08 Å but equal to the reported value in a recent study using a similar computational approach [17]. The supercell approach is used to describe the surface, with each repeat unit containing nine silver atoms in a 3×3 pattern in each of six layers. Along the (111) direction, the $3 \times 3 \times 6$ slabs are separated by a vacuum spacing of six interlayer distances (14.4 Å). The rather large in-plane unit cell for a 3×3 pattern partially reduces image and lateral interactions between adsorbed molecules. In computing the total energy, integrations over the first Brillouin zone are performed by discrete summations on a finite number of k-points. We use the standard Monkhorst–Pack [21] grid ($3 \times 3 \times 1$ sampling mesh), which is reduced by time-reversal symmetry to an irreducible set of five weighted sampling points. The two top layers of the bare silver slab are fully relaxed. A molecule is then positioned on a binding site on the surface, and simultaneous relaxation of the structure of the adsorbate and the two top layers of the metallic slab are performed until the self-consistent forces are lower than 0.05 eV Å^{-1}. For all total energies reported here, the zero of energy is chosen to be the energy of infinitely separated neutral atoms.

The clean silver surface is first characterized for establishing the accuracy of the calculation. In particular, three parameters are examined for validating the description of the silver surface and the bulk: the density of k-point sampling, the number of silver layers (N), and the number of vacuum layers between slabs. Using the preferred method [22, 23], the total energy is computed for slabs with increasing numbers of layers until convergence is achieved for the bulk energy. The slab energy is then computed for the evaluation of the surface energy. We perform these tests using the $1 \times 1 \times N$ slab, i.e. N layers with the primitive surface cell, keeping the vacuum space constant at six layers. Two sets of k-points are chosen for the test

Table 1. The convergence of the surface energy E_{surf} per primitive cell and the work function Φ (in eV) of the Ag(111) surface as a function of the number of layers N, using two sets of k-points.

	k-sampling: $9 \times 9 \times 1$				k-sampling: $15 \times 15 \times 1$			
N	$E_{slab}(N)$	$E_{bulk}(N)$	$E_{surf}(N)$	Φ	$E_{slab}(N)$	$E_{bulk}(N)$	$E_{surf}(N)$	Φ
4	−10.196	−2.727	0.356	4.441	−10.186	−2.714	0.335	4.486
5	−12.921	−2.725	0.352	4.421	−12.908	−2.723	0.353	4.456
6	−15.638	−2.716	0.329	4.396	−15.626	−2.718	0.341	4.433
7	−18.368	−2.730	0.371	4.363	−18.344	−2.718	0.341	4.419
8	−21.080	−2.712	0.309	4.353				
9	−23.810	−2.729	0.378	4.347				
10	−26.526	−2.716	0.319	4.345				
11	−29.243	−2.717	0.321	4.350				

calculations: $9 \times 9 \times 1$ (equivalent to $3 \times 3 \times 1$ k-point sampling for the $3 \times 3 \times 6$ unit cell of the adsorbate system) and $15 \times 15 \times 1$. The results are summarized in table 1. With the finer $15 \times 15 \times 1$ sampling, convergence is achieved at $N = 6$, giving a surface energy per primitive cell area of 0.341 eV. This number agrees with the 0.34 eV per surface atom value reported in [24] and compares well with the similar calculations in [25], which determined a surface energy of 0.59 eV per 1×1 (001) area. The latter value corresponds to a surface energy of 0.34 eV per 1×1 (111) area, in excellent agreement with our result. With the $9 \times 9 \times 1$ k-sampling, complete convergence requires $N = 10$. The six-layer slab is chosen for the physisorption studies since it gives a bulk value very close to the converged value of −2.716 eV per atom and a 1×1 (111) surface energy of 0.329 eV with an acceptable error bar of 3.5%.

This $1 \times 1 \times N$ system has also been used to evaluate the work function. From experiments, a work function value of 4.46 ± 0.2 eV was determined [26] for Ag(111). By definition the work function is the minimum energy required to extract one electron to an infinite distance from the surface. It is computed here as the difference between the electrostatic potential in the middle of the vacuum region and the Fermi energy of our slab. Since at the calculated distance of 3–5 layers from the surface the electrostatic image force of a free electron cannot be neglected, our calculated value should be somewhat lower than the experimental number. Table 1 shows that the calculated work function converges to 4.42 eV for the $15 \times 15 \times 1$ k-grid and to 4.35 eV for the $9 \times 9 \times 1$ k-grid. The six-layer slab appears to provide a good compromise between accuracy [27] and time consumption for simulating bulk silver. Furthermore, the effect of vacuum space in this calculation has been examined and no change is observed when vacuum space wider than six layers is used.

In modelling physisorption, three different sites on the Ag(111) surface (fcc hollow, bridge and top) and two orientations of the carbon-carbon double bond relative to the Ag atom rows (parallel and perpendicular) have been used to construct initial adsorption geometries. These different starting configurations all yield identical relaxed adsorption structures and binding energies for all three molecules.

2.2. *Adsorption structure*

The lowest energy adsorption configurations of the three systems, depicted in figure 1, all have molecular structures that are essentially identical to their gas-phase structures. The preferred adsorption position of ethylene is the top site, while VC adsorbs at the bridge and butadiene adsorbs with its double bonds on two adjacent top sites. Both ethylene and butadiene lie flat on the surface. VC adopts a tilted orientation, with the centre of chlorine atom repelled from the surface. The tilted orientation of the VC molecular plane can be described by two angles: $\theta = 10^\circ$ between the C–C bond and the surface plane and a molecular rotation angle $\alpha = 20^\circ$ around the C–C bond. This orientation compares with the experimental results of $\theta = 26^\circ$ and $\alpha = 33^\circ$. The distances between the molecular center of mass and the nearest surface silver atom are calculated to be between 3 and 3.5 Å, with butadiene and ethylene somewhat closer the surface than VC.

The gas-phase-like structures of the adsorbate molecules reflect non-covalent adsorbate–substrate bonding, i.e. no significant electron density between adsorbate and substrate. The molecular orientation parallel to the surface allows ethylene and butadiene to maximize their interactions between the metal and the π electrons. By contrast, VC tilts to accommodate the large chlorine atom. The resulting structures of the three systems balance gentle adsorbate–substrate interactions and steric effects.

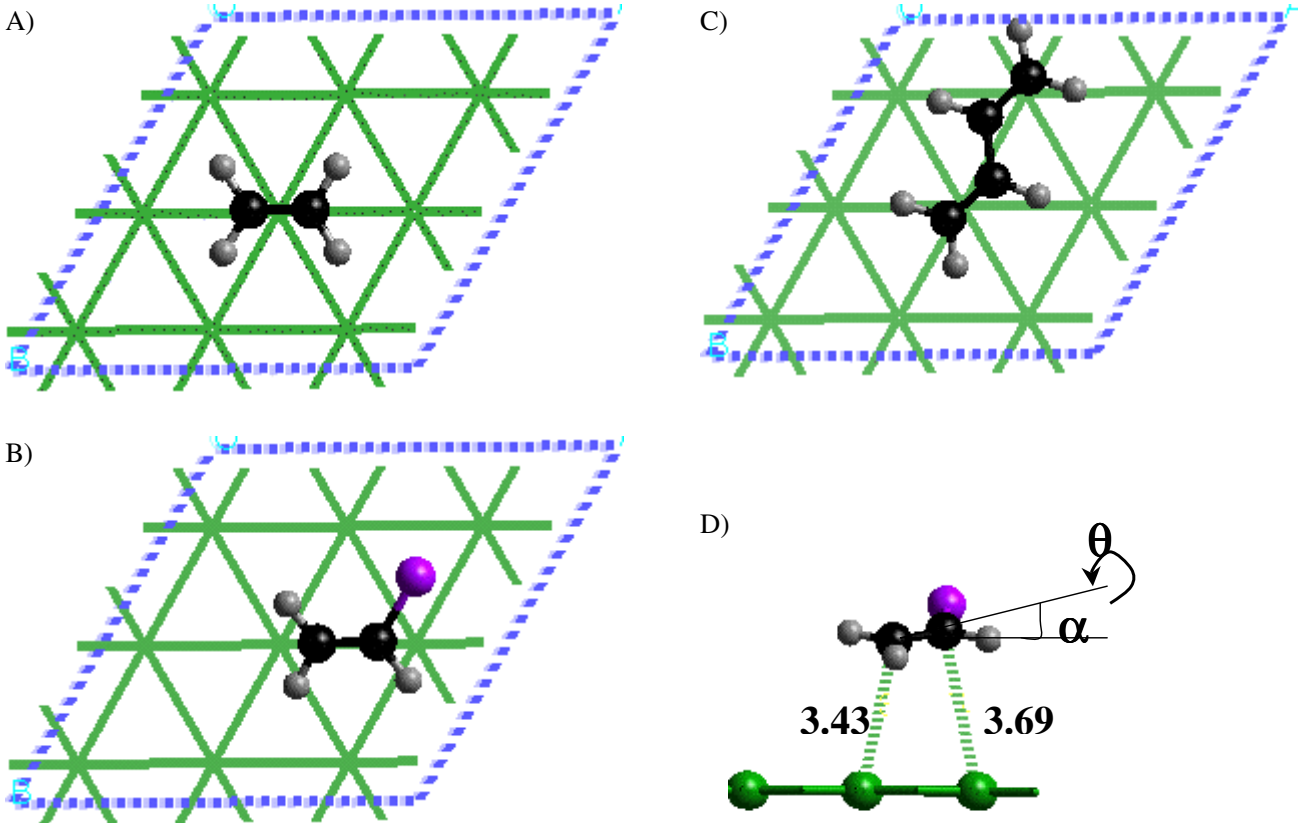

Figure 1. Relaxed structures obtained for ethylene on top (A), VC on bridge (B) and butadiene on top-top (C) adsorbed on Ag(111) in a $p(3 \times 3)$ unit cell. The supercell is indicated by broken lines. Panel D shows the tilted orientation of VC molecular plane, described by two angles: $\theta = 10°$ between the C═C bond and substrate plane and $\alpha = 20°$, the molecular rotation angle around the C═C bond.

2.3. *Binding energy*

The adsorption energy E_a at a specific coverage is the difference between the total energy of the adsorbed system and those of the clean substrate and the gas phase molecule (labelled 'mol'). This adsorption energy E_a can be further separated into two contributions: the binding energy (BE) characterizing the interaction of an isolated adsorbate molecule with the metal, and $E_{\text{inter-ad}}$ that accounts for intermolecular interactions between adsorbate molecules. $E_{\text{inter-ad}}$ can be evaluated as the difference in total energy between an array of molecules in the adsorption geometry (without the substrate) and the same number of isolated molecules, both calculated in a large cubic supercell (of length 17 Å). Subsequently, BE can be computed as the difference between E_a and $E_{\text{inter-ad}}$.

The binding energies of the molecules on Ag(111) in the 3×3 unit cell are shown in table 2. All the calculated binding energies for the molecules on silver are, not surprisingly, far smaller than experiment. In order to compare with experimental data, we note that it is the desorption energy E_d which is experimentally measured in thermal desorption spectroscopy. This quantity is an activation energy associated with a kinetic process, whereas the computed BE is a thermodynamic quantity at 0 K. Transition state theory allows correlation between these two values as $E_d = \text{BE} + RT$. RT varies between 0.22 and 0.33 kcal mol^{-1} for the temperature range of the desorption peaks. This entropy contribution adds to the BE value but does not fill

Table 2. Binding energy (BE) and silver work function change ($\Delta\Phi$) induced by the three alkenes on the Ag(111) surface. The work function change is calculated for the situation where there is one molecule in a 3×3 unit cell. BE values in parentheses include the RT correction for comparison with experimental desorption energies.

Adsorbate	BE (kcal mol^{-1})	$\Delta\Phi$ (eV, for a 3×3 cell)
Vinyl chloride	0.8 (1.0)	+0.004
Ethylene	1.5 (1.8)	−0.17
Butadiene	0.8 (1.1)	−0.30

the gap between experiment and theory. The results show that although current standard implementations of DFT without long range dispersion forces [28] can be successful for binding energies of strongly-bonded chemisorbed species, they are inadequate for dealing with the binding energies of weakly bound, physisorbed species on metals.

2.4. *Adsorbate induced work function change*

The work function decrease ($\Delta\Phi$) of Ag(111) induced by the adsorption of the three molecules, with one molecule each in a 3×3 cell, are shown in table 2. The work function change for ethylene on Ag(111) has been measured at saturation coverage as $\Delta\Phi = -0.38$ eV [9]. From our calculations, $\Delta\Phi$ for ethylene at saturation coverage can be extrapolated from the calculated $\Delta\Phi$ at half-monolayer coverage (-0.207 eV, calculated with a 2×2 cell) by multiplying by 2 to yield –0.41 eV. This is a slight overestimate, but very close to the measured value. Unfortunately, $\Delta\Phi$ values for VC and butadiene on Ag(111) have not been experimentally determined. Ref. [7] suggests that larger induced work function changes correlate to higher desorption temperatures, and so experimental TDS results lead us to expect that the work function change should increase from VC to ethylene to butadiene.

3. Discussion

It is interesting to see from table 2 that the theoretically computed $\Delta\Phi$ values display a trend of increase from VC (0.0 eV) to ethylene (0.17 eV) to butadiene (0.30 eV). This trend is in line with the observed desorption temperatures (110 K, 128 K, and 166 K), which are related to the binding energies on the surface. DFT calculations are apparently more successful in predicting the magnitude of adsorption induced work function change $\Delta\Phi$ than binding energies for physisorbed systems. We propose below a model based on molecular orbitals for the interpretation of the trend of $\Delta\Phi$ among the three systems. This model may also provide insight into understanding the nature of the bonding between the three olefins and silver. Through out this model we explore the potential of using $\Delta\Phi$ calculated by DFT for examining the relative binding strength in physisorbed systems.

$\Delta\Phi$ can be rationalized from the formation of an interface dipole upon molecular adsorption. The sign of $\Delta\Phi$ correlates with the direction of this interface dipole. The lowering of the work function then corresponds to a dipole pointing outward. $\Delta\Phi$ can be divided into two contributions: a covalent 'chemical' term stemming from short-range bonding, and an electrostatic 'physical' term from long-range interactions. A recent study [29] has examined these two contributions and indicated that the chemical part reflects the charge transfer upon adsorption while the physical part represents the surface metal electron density tail induced by the presence of adsorbed species. For physisorbed species it is anticipated that the chemical contribution is negligible and the physical contribution dominates. In order to assert the contribution of the covalent term, we examine the self-consistent density of one-electron states (DOS) of the adsorbed molecules on Ag(111), which is plotted in figure 2. The *d* band of silver lies between -6 and -2.5 eV. The small features above the *d* band arise from the *sp* states of silver. For butadiene and VC, all the molecular electron density peaks remain sharp and match exactly with their gas-phase counter parts. The absence of broadening or shift of the molecular states clearly indicates non-covalent adsorption for these two molecules excluding any charge transfer. The situation is somewhat different for ethylene, since its π level around -4 to -3 eV is significantly broadened and displays a doublet structure that is characteristic of bonding and anti-bonding interactions with the metal *d* bands. In fact, the ethylene π level lies just below the top of the *d* band, enabling resonant mixing. This apparent mixing involving ethylene π orbital may give rise to a slight donation of the π electrons toward the metal and would partly explain the work function decrease induced by ethylene adsorption.

Figure 3 is a summary of the π level positions of the three molecules in the gas phase and their interactions with the metal orbitals. This data provides a semi-quantitative picture for understanding the non-covalent bonding of the ethylene derivatives with silver. The π and π^* levels of ethylene are symmetrically displaced by 2.75 eV from the carbon atomic 2*p* level. For VC, the frontier orbitals are affected by the presence of chlorine, which delocalizes the conjugate π electron density. A three-level coupling scheme for VC molecular orbitals is illustrated in figure 3; the HOMO of VC results principally from an anti-bonding interaction between the low lying 2*p* level of Cl and the π level of the C=C chromophore, and the 2*p* (Cl) also has a lesser anti-bonding interaction with the LUMO π^* level. The butadiene frontier orbitals can be constructed from a four-level orbital scheme involving the two interacting vinyl fragments. The main interactions are between degenerate levels: the two π levels and the two π^* levels respectively. We have shown only the two frontier levels symmetrically located at 2 eV around the non-bonding level. Thus, going from ethylene to VC to butadiene, the HOMO levels are shifted up, becoming farther off resonance with the low-lying Ag *d* band. The tilted adsorption structure of VC also is consistent with lesser overlap of π orbital with the metal beneath.

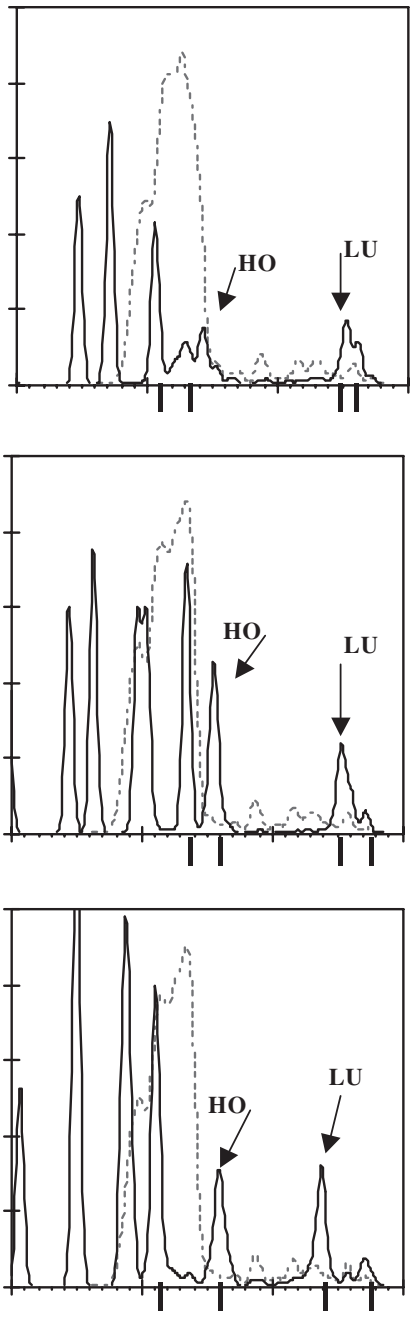

Figure 2. Self-consistent projected density of states (DOS) as function of energy of the Ag(111) surface atoms (broken line) together with those of the adsorbed molecule (full line): (top) ethylene, (middle) vinyl chloride, and (bottom) butadiene. The Fermi level located between HOMO (HO) and LUMO (LU) orbitals of each adsorbate is indicated by a small black mark on the energy X axis. Larger marks at the bottom indicate as reference levels the corresponding orbitals of the gas phase.

The covalent interaction is consequently slightly bonding for ethylene and non-bonding for the other two derivatives, as reflected in the DFT calculated BE of table 2.

The electrostatic interaction energy can be shown to correlate with the interface dipole. For polar molecules, there is an electrostatic attraction between the molecular dipole and its classical image in the metal. For the tilted VC, its dipole has a small component that points into the surface. The second part of the interaction, which is the only source for non-polar molecules, comes from the attraction between the polarizability of the molecule and its induced image charge in the metal. The role of dispersion forces in the interaction of ethylene on silver has recently been analysed [30] and dispersion forces have recently been pictured with DFT charge density differences for benzene on Al(111) [31]. For all molecules under consideration here, this polarizability would include a small amount of charge transfer from molecule to metal, giving a surface dipole pointing outward and causing the work function to decrease. For VC, it is possible that the two dipoles, the molecular and the induced surface dipoles, offset each other and result in a near zero, but positive $\Delta\Phi$. The polarizability of butadiene must be higher than that of ethylene, because the electron density of butadiene is more accessible (HOMO is closer to the vacuum level than that of ethylene). In addition, the lower-lying LUMO of butadiene would enhance the magnitude of the induced dipole, since it originates from quantum mixing between the excited and the ground states [32]. The higher polarizability increases the magnitude of $\Delta\Phi$ for butadiene compared to ethylene, as is found in our calculations.

In summary, it appears that the polarizability associated with the π electrons, in a non-covalent, electrostatic, off-resonance coupling with the *d* band of silver, predominantly determines the strength of the adsorbate–substrate interaction and is mainly responsible for the work function change of the silver surface.

Even though our analysis is qualitatively satisfactory in explaining the correlation between the BE and work function change, one still needs to address the apparent paradox—why the GGA based DFT calculation, where long-range interaction is intrinsically excluded, can produce the work function change which arises mainly from long-range interactions? The work by Bagus *et al.* [33] provides a new insight into this problem. In a computational Hartree–Fock SCF study using second-order perturbation theory (MP2) to include vdW dispersion forces, they showed that the surface dipole associated with molecules physisorbed on metals does not originate from the two contributions discussed above but rather from a quantum effect related to the anti-symmetrization of the electronic wave functions

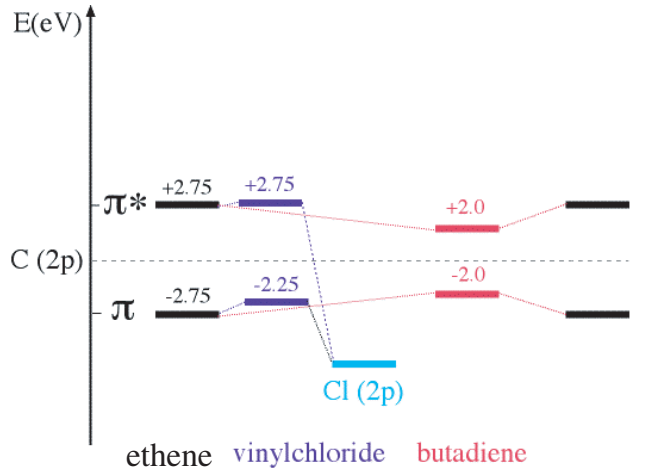

Figure 3. Schematic orbital diagram showing the relative positions of the HOMO and LUMO orbitals of ethylene, VC, and butadiene. Numerical values above orbitals correspond to their energies in eV relative to the non-bonding atomic level (dotted line) deduced from figure 2.

(exchange-like mechanism depicted as the exchange interaction energy). In the DFT calculations this fermion property is actually included. It is therefore not surprising that $\Delta\Phi$ can be reproduced within our DFT model calculation.

4. Concluding remarks

The DFT-GGA calculations presented in this study show that this approach is capable of justifying the structures of physisorbed states as resulted from a combination of steric and long-range interaction effects. Though this DFT approach is not successful in reproducing the adsorption energies—the calculated binding energies are all much smaller than the experimental values—it does produce a trend for the adsorption induced substrate work function change that correlates with the experimentally observed adsorbate–substrate binding energies. The recent work of Bagus *et al.* [33] has pointed out that the interface dipole is mostly responsible for the work function change and is a quantity not much affected by the long range forces. This is probably why such DFT calculations can still produce reasonable work function changes induced by adsorption in physisorbed systems. The observation made in this study suggest that perhaps DFT calculations can be used to gauge the molecule–substrate binding energy, at least on relative scale, in physisorbed systems through examining the adsorbate induced work function change. The correlation observed between the calculated work function change and the binding energy also calls for more experimental measurements on the relationship among the two physical quantities.

This report is based on the work completed when MLB was visiting the University of Pennsylvania. During the submission of this report we have noticed the paper on DFT calculation of alkane adsorption on metal [34], which also showed that adsorption induced work function change can be reproduced by DFT-GGA.

Acknowledgement

The authors thank Dr Yashar Yourdshahyan for advice relating to surface energy calculations, and Drs J. S. Filhol and D. Pursell for stimulating discussions. This work is supported in part by the NSF MRSEC programme under grant DMR00-79909. AMR and HLD acknowledge support from the Air Force Office of Scientific Research, Air Force Materiel Command, USAF, under grant numbers FA9550-04-1-0077 and F49620-01-1-0517, respectively.

References

[1] (a) S.P. Lewis, A.M. Rappe, *J. Chem. Phys.*, **110,** 4619 (1990); (b) N. Lorente, M.F.G. Hedouin, R.E. Palmer, M. Persson, *Phys. Rev.* B, **68,** 155401 (2003).
[2] W. Kohn, Y. Meir, D.E. Makarov, *Phys. Rev. Lett.*, **80,** 4153 (1998).
[3] Y. Andersson, D.C. Langreth, B.I. Lundqvist, *Phys. Rev. Lett.*, **76,** 102 (1995).
[4] (a) H. Rydberg, *et al.*, *Phys. Rev. Lett.*, **91,** 126402 (2003); (b) C. Adamo, V. Barone, *J. Chem. Phys.*, **108,** 664 (1998).
[5] (a) C. Tuma, A. Daniel Boese, N.C. Handy, *Phys. Chem. Chem. Phys.*, **1,** 3939 (1999); (b) T. Yanai, D.P. Tew, N.C. Handy, *Chem. Phys. Lett.*, **393,** 51 (2004).
[6] (a) J.P. Perdew, S. Kurth, A. Zupan, P. Blaha, *Phys. Rev. Lett.*, **82,** 2544, 5179 (1999); (b) S. Kurth, J.P. Perdew, P. Blaha, *Int. J. Quantum Chem.*, **75,** 889 (1999).
[7] T. Livneh, Y. Lilach, M. Asscher, *J. Chem. Phys.*, **111,** 11138 (1999).
[8] D.P. Pursell, M.-L. Bocquet, J.M. Vohs, H.-L. Dai, *Surf. Sci.*, **522,** 90 (2003).
[9] X.-L. Zhou, J.M. White, *J. Phys. Chem.*, **96,** 7703 (1992).
[10] (a) P.-A. Redhead, *Vacuum*, **12,** 203 (1962); (b) X.-L. Zhou, J.M. White, B.E. Koel, *Surf. Sci.*, **218,** 201 (1989).
[11] D.H. Parker, M.E. Jones, B.E. Koel, *Surf. Sci.*, **233,** 65 (1990).
[12] E.A. Carter, W.A. Goddard, *Surf. Sci.*, **209,** 243 (1989).
[13] P.J. van den Hoek, E.J. Baerends, R.A. van Santen, *J. Phys. Chem.*, **93,** 6469 (1989).
[14] H. Kobayashi, K. Nakashiro, T. Iwakuwa, *Theor. Chem. Acc.*, **102,** 237 (1999).
[15] K.A. Jorgensen, R. Hoffmann, *J. Phys. Chem.*, **94,** 3046 (1990).
[16] C. Backx, C.P.M. de Groot, P. Biloen, W.M.H. Sachtler, *Surf. Sci.*, **128,** 81 (1983).
[17] A. Kokalj, A. Dal Corso, S. de Gironcoli, S. Baroni, *Surf. Sci.*, **62,** 507 (2002).

[18] (a) G. Kresse, J. Hafner, *Phys. Rev.* B, **47,** RC558 (1993); (b) G. Kresse, J. Furthmuller, *Comput. Mater. Sci.*, **6,** 15 (1996); (c) G. Kresse, J. Furthmuller, *Phys. Rev.* B, **54,** 11169 (1994).
[19] D.H. Vanderbilt, *Phys. Rev.* B, **41,** 7892 (1990).
[20] J.P. Perdew, Y. Wang, *Phys. Rev.* B, **45,** 13244 (1992).
[21] H.J. Monkhorst, J.D. Pack, *Phys. Rev.* B, **13,** 5188 (1976).
[22] (a) J.C. Boettger, S.B. Trickey, *Phys. Rev.* B, **45,** 1363 (1992); (b) J.C. Boettger, *Phys. Rev.* B, **49,** 16798 (1994).
[23] K. Doll, N.M. Harrison, *Chem. Phys. Lett.*, **317,** 282 (2000).
[24] N.H. de Leeuw, C.J. Nelson, *J. Phys. Chem.* B, **107,** 3528 (2003).
[25] V. Fiorentini, M. Methfessel, M. Scheffler, *Phys. Rev. Lett.*, **71,** 1051 (1993).
[26] M. Chelvayohan, C.H.B. Mee, *J. Phys. C: Solid. State Phys.*, **15,** 2305 (1982).
[27] The theoretical quantum size effect (on the order of < 0.1 eV) referred to in C.J. Fall, N. Binggeli, A. Baldereschi, *J. Phys.: Condens. Matter*, **11,** 2689 has been ignored (1989).
[28] N.D. Lang, *Phys. Rev. Lett.*, **46,** 842 (1981).
[29] X. Crispin, V.M. Geskin, A. Crispin, J. Cornil, R. Lazzaroni, W.R. Salaneck, J.L. Brédas, *J. Am. Chem. Soc.*, **124,** 8131 (2002).
[30] G. Katz, Y. Zeiri, R. Kosloff, *Surf. Sci.*, **425,** 1 (1999).
[31] R. Duschek, F. Mittendorfer, R.I.R. Blyth, F.P. Netzer, J. Hafner, M.G. Ramsey, *Chem. Phys. Lett.*, **318,** 43 (2000).
[32] A. Zangwill, *Physics at Surfaces*, Cambridge University Press, Cambridge (1988).
[33] P.S. Bagus, V. Staemmler, C. Wöll, *Phys. Rev. Lett.*, **89,** 096104 (2002).
[34] Y. Morikawa, H. Ishii, K. Seki, *Phys. Rev.* B, **69,** 041403 (R) (2004).